



Published in final edited form as:

Science. 2009 December 4; 326(5958): 1406–1410. doi:10.1126/science.1178712.

## Planarian Hh signaling regulates regeneration polarity and links Hh pathway evolution to cilia

Jochen C. Rink<sup>\*</sup>, Kyle A. Gurley<sup>\*</sup>, Sarah A. Elliott, and Alejandro Sánchez Alvarado<sup>¶</sup>

Department of Neurobiology & Anatomy, Howard Hughes Medical Institute, University of Utah School of Medicine, 401 MREB, 20 North 1900 East, Salt Lake City, UT 84103

### Abstract

The Hedgehog (Hh) signaling pathway plays multiple essential roles during metazoan development, homeostasis, and disease. Although core protein components are highly conserved, the variations in Hh signal transduction mechanisms exhibited by existing model systems (*Drosophila*, fish, and mammals) are difficult to understand. We characterize the Hh pathway in planarians. Hh signaling is essential for establishing the Anterior/Posterior axis during regeneration by modulating *wnt* expression. Moreover, RNAi methods to reduce signal transduction proteins *Cos2/Kif27/Kif7*, *Fused*, or *Iguana* do not result in detectable Hh signaling defects; however, these proteins are essential for planarian ciliogenesis. Our study expands the understanding of Hh signaling in the animal kingdom and suggests an ancestral mechanistic link between Hh signaling and the function of cilia.

The Hh signaling pathway plays numerous evolutionarily conserved roles in the regulation of cell growth and patterning during the embryonic and postembryonic development of animals as diverse as fruitflies and humans. The misregulation of this pathway has equally profound consequences resulting in defects such as holoprosencephaly (cyclopia) and tumorigenesis. Secreted Hh protein alters gene transcription by binding the cell-surface receptor Patched (Ptc), preventing repression of the 7 membrane spanning receptor Smoothed (Smo) by Ptc. This activates Gli transcription factors and inactivates their inhibitor Suppressor of Fused (SuFu). Despite conservation of these core components and their mode of function (1,2), Hh signal transduction mechanisms appear to have diversified throughout evolution (3). *Drosophila* Hh signaling is cilia-independent and requires the kinesin Costal2 (4) (Kif7/27 in vertebrates) and the kinase Fused (5). The mouse Hh pathway requires primary cilia (6,7) and Kif7 (8–10), but not Fused (11,12). Zebrafish utilize cilia, Kif7, Fused, and Iguana/Dzip1 (Igu) (13–19). *C. elegans* has lost a functional Hh pathway altogether (20). Since planarians belong to a group of animals that evolved independently from flies, fish, and mammals (Sup. Fig. 1) an analysis of planarian Hh signaling could reveal how the mechanistic differences in a highly conserved signaling pathway arose.

Systematic sequence homology searching of the *S. mediterranea* genome identified single homologs for planarian Hh (*Smed-hh*), Patched (*Smed-ptc*), Smoothed (*Smed-smo*) and Suppressor of Fused (*Smed-sufu*), but three Gli homologs (37) (Sup. Fig. 2,3). Of the Gli homologs, only *Smed-gli-1* exhibited an obvious role in Hh signaling (see below). We cloned (see SOM) and analyzed the expression of these planarian Hh components by in-situ hybridization (Fig. 1A–C, Sup. Fig. 4). *ptc* expression was reduced by RNAi of pathway activators (*hh*, *smo*, *gli-1*) and elevated by RNAi of pathway inhibitors (*ptc*, *sufu*) (Fig. 1B), suggesting that as in other animals (21–23), *ptc* is a Hh target in planarians and its expression

<sup>¶</sup>To whom correspondence should be addressed: [sanchez@neuro.utah.edu](mailto:sanchez@neuro.utah.edu).  
Authors contributed equally to this work

marks sites of Hh signaling. Complementary expression of *ptc*, *hh*, and *smo* throughout the central nervous system (CNS), and *hh*, *ptc*, *smo*, *sufu*, and *gli-1* near the root of the pharynx implicates these locations as possible sites of Hh activity (Fig. 1A, Sup. Fig. 4). *gli-1* expression in cells surrounding the gut enterocytes (Fig. 1A) and particularly strong *ptc* upregulation upon *sufu(RNAi)* in the same region (Fig. 1C) may indicate a conserved function of Hh in the gastrovascular system (24,25). Additionally, mitotic activity was increased by *ptc(RNAi)* and *sufu(RNAi)*, but decreased by *hh(RNAi)* (Sup. Fig. 5, 6), mirroring the mitotic effects of Hh in other organisms (26,27). Altogether, these initial studies suggest that planarian Hh signaling likely has diverse functions in various adult tissues.

To test whether the Hh pathway contributes to the signaling network orchestrating planarian regeneration, we amputated the heads and tails of dsRNA-fed animals. Targeting the pathway activator *hh* left anterior regeneration unaffected, but caused a range of posterior regeneration defects including reduced or absent tail tissue and concomitant changes in posterior marker expression (Fig. 2A-B", Sup. Fig. 7). Conversely, RNAi against the pathway inhibitor *ptc* left posterior regeneration unaffected, but caused anterior specific defects, including tail instead of head formation and striking changes in marker expression (Fig. 2D-F", Sup. Fig. 7; Sup. Movies 1 and 2). Targeting *gli-1* and *smo* produced identical regeneration phenotypes to *hh (RNAi)*, and *sufu(RNAi)* resembled *ptc(RNAi)* (Sup. Fig. 8), establishing tail or head regeneration defects as general consequence of decreased or increased Hh signaling, respectively. Systematic RNAi-dosage experiments ranked the range of phenotypes according to severity. Three observations are particularly noteworthy. First, "headless" animals expressed neither head nor tail markers anteriorly (Fig. 2E', E"), but expressed a marker for intermediate anterior cell fate (Sup. Fig. 9), reminiscent of dose-dependent roles for Hh in other contexts (28). Second, "cyclopic" animals resulted from increased Hh signaling. The same phenotype occurs in vertebrates (29), but is caused by decreased Hh signaling. This difference, along with lack of expression of *Smed-hh* along the planarian midline, suggests that the midline function of Hh in vertebrates is not conserved in planarians. Third, SuFu has a prominent role in planarians, which is similar to vertebrates but different from *Drosophila* (30). RNAi-combination of two pathway activators or inhibitors enhanced the respective phenotypes whereas activator-inhibitor combinations suppressed each other (Sup. Fig. 10). However, besides the expected and predominant function of Smo as a pathway activator, these experiments also indicated a cryptic inhibitory activity, but the mechanistic basis of this effect is currently unclear. Combined with regeneration time course experiments showing that Hh-related phenotypes originate during early phases of regeneration (Sup. Fig. 11), our data demonstrate that the different phenotypic classes resulting from altered Hh signaling constitute a series of A/P patterning defects, and that early Hh signaling is necessary and sufficient for tail regeneration.

The early requirements for elevated Hh signaling in tails and reduced Hh signaling in heads mirrors those for  $\beta$ -catenin signaling (31–33). In addition, diluted dosages of *APC-1(RNAi)*, which elevate  $\beta$ -catenin activity (31) produced a range of phenotypes remarkably similar to *ptc (RNAi)* (Sup. Fig. 12). Combining doses of *ptc(RNAi)* and *APC-1(RNAi)* that by themselves elicited only weak defects led to a striking increase in phenotype severity (Fig. 3A). Moreover, a single feeding of  *$\beta$ catenin-1(RNAi)* in *ptc(RNAi)*-fed animals completely suppressed the *ptc (RNAi)* "two-tail" phenotype, causing head formation at both anterior and posterior wounds (Fig. 3B). Thus, the Hh and  $\beta$ -catenin pathways synergize functionally to specify tails, and tail induction by elevated Hh signaling depends on  $\beta$ -catenin activity.

Because a Wnt ligand (*Smed-wntP-1*) was recently implicated in activating  $\beta$ -catenin during tail regeneration (34), we examined whether *wnt* expression was regulated by Hh signaling. One day after amputation, *wntP-1* expression was reduced in *hh(RNAi)* animals and strongly increased in *ptc(RNAi)* animals (Fig. 3C, top). In contrast, *wntP-1* expression was not altered

in *βcatenin-1(RNAi)* or *APC-1(RNAi)* animals (Fig. 3C, bottom), ruling out indirect polarity-associated effects. Expression of an additional *wnt* gene functioning in tail regeneration (*Smed-wnt11-2*) (34), showed a dependence on both Hh and  $\beta$ -catenin pathway activity (Sup. Fig. 13). Unchanged *ptc* expression in *βcatenin-1(RNAi)* or *APC-1(RNAi)* animals suggested that  $\beta$ -catenin may not reciprocally control Hh signaling (Sup. Fig. 14). *wntP-1(RNAi)* suppressed the *ptc(RNAi)* phenotypes at anterior wounds (Fig. 3D) and strongly enhanced the *hh(RNAi)* phenotypes at posterior wounds, synergistically leading to the appearance of a posterior head in 20% of *wntP-1(RNAi);hh(RNAi)* animals (Fig. 3E). These data indicate that Hh-mediated *wntP-1* expression is likely responsible for the posteriorizing effect of *ptc(RNAi)* and that improved *hh(RNAi)* efficiency might be sufficient for head formation from posterior wounds. In intact animals, *wnt* expression did not respond to alterations of Hh pathway activity (Sup. Fig. 15), suggesting that Hh control of *wnt* expression is specific to the establishment of A/P polarity during regeneration.

The expression patterns of *hh*, *ptc*, and *wnt-P1* did not show a posterior bias as might be expected from their requirement for tail formation (Fig. 3C; Sup. Fig. 16). Whereas such bias could be short-lived or difficult to detect, symmetric Hh activity and *wnt* expression would require additional components to specifically inhibit  $\beta$ -catenin activity anteriorly. Nonetheless, our data clearly demonstrate synergies between the Hh and Wnt signaling pathways during regeneration. We conclude that Hh influences A/P fate by controlling *wnt* expression.

The range of Hh-related regeneration defects from subtle to severe (Fig. 2) provided a sensitive readout to assess whether cilia or other signal transduction components play a role in the planarian Hh pathway. We cloned planarian homologs of intraflagellar transport (IFT) proteins (37) (*Smed-IFT52*, *Smed-IFT88*, *Smed-IFT172*, *Smed-kif3b*; Sup. Fig. 17), which are universally required for the assembly of cilia (35). Animals fed dsRNA targeting any of the IFT-components lost their cilia-dependent gliding ability, advancing more slowly by waves of whole-body contraction and extension (inchworming) instead (Fig. 4A, Sup. Fig. 18, Sup. Movie 3). Consistently, their cilia were severely shortened (Fig. 4B). Additionally, *IFT(RNAi)* animals developed edema (inset Fig. 4A), likely due to impaired osmoregulation by their heavily ciliated protonephridia. Targeting Hh pathway components did not affect cilia (Fig. 4A,B). Despite the prominent cilia defects, *IFT(RNAi)*-treated animals showed no evidence of altered Hh signaling during regeneration by morphology and early marker expression (Sup. Fig. 19), and *ptc* expression was unaffected in the CNS, pharynx, and gut (Sup. Fig. 20A). Although we cannot entirely exclude subtle, non-regeneration related, or residual cilia contributions (17), our data did not uncover a role for cilia in planarian Hh signaling.

We next cloned the single planarian homologs of Fused (*Smed-fused*), Cos2/Kif27/Kif7 (*Smed-kif27*), and Iguana (*Smed-iguana*) (37) (Sup. Fig. 17), which were all discovered as mutations severely affecting Hh signaling in *Drosophila* (4,5) or zebrafish (18,19), respectively. Silencing *fused*, *kif27*, or *iguana* neither perturbed *ptc* expression (Sup. Fig. 20B), nor did it elicit Hh-related regeneration defects (Sup. Fig. 21). Hence these components are unlikely to function in planarian Hh signaling, but the same caveat raised for the IFT genes applies. Intriguingly, *fused(RNAi)*, *kif27(RNAi)*, or *iguana(RNAi)*-treated worms instead displayed compromised mobility (Fig. 4C), inchworming, tissue edema (Fig. 4D) and complete lack of cilia staining (Fig. 4E). Furthermore, the expression patterns of *iguana* and *kif27* closely resembled those of cilia genes (Sup. Fig. 22). These data demonstrate by multiple functional and morphological criteria, that *fused*, *kif27*, and *iguana* are essential for planarian ciliogenesis.

This finding establishes that the ciliogenesis functions of Fused, Kif7, and Iguana are not vertebrate-specific (15,17), but instead ancestral. The use of cilia, Fused, Kif7, and Iguana in the zebrafish Hh pathway (13–15,18,19), cilia and Kif7 in the mouse Hh pathway (8–10), and

Fused and Cos2 in the *Drosophila* Hh pathway (3) further implies that all three model organisms rely on cilia and/or ancient cilia components for Hh signaling. Thus, the association between Hh signaling and cilia is most likely also ancestral (Sup. Fig. 23). This conclusion is based solely on the ciliogenesis functions of Fused, Cos2/Kif27/Kif7, and Iguana and is unaffected by whether they also function in planarian Hh signaling. In fact, uncovering evidence to this effect would further strengthen the argument for an ancestral connection.

Our findings suggest that the perplexing diversity in Hh signal transduction mechanisms among flies, fish, and mammals arose from group-specific losses of the ancestral association between cilia and Hh signaling (Sup. Fig. 23). This raises the question why core components are highly conserved, yet the contribution of cilia-related proteins to Hh signaling is variable. The dynamic shuttling of core components between subcellular compartments in both flies and vertebrates (9, 10, 36) may have originally been organized by cilia (providing a location) and the associated IFT complexes (providing the motors). The divergence of Hh signaling mechanisms could thus reflect the choice of a new location or motor for organizing the interplay between core components.

## Supplementary Material

Refer to Web version on PubMed Central for supplementary material.

## REFERENCES AND NOTES

- Ingham PW, Placzek M. Nature reviews Nov;2006 7:841.
- Lum L, Beachy PA. Science Jun 18;2004 304:1755. [PubMed: 15205520]
- Huangfu D, Anderson KV. Development Jan;2006 133:3. [PubMed: 16339192]
- Sisson JC, Ho KS, Suyama K, Scott MP. Cell Jul 25;1997 90:235. [PubMed: 9244298]
- Preat T, et al. Nature Sep 6;1990 347:87. [PubMed: 2168522]
- Huangfu D, Anderson KV. Proc Natl Acad Sci U S A Aug 9;2005 102:11325. [PubMed: 16061793]
- Huangfu D, et al. Nature Nov 6;2003 426:83. [PubMed: 14603322]
- Cheung HO, et al. Sci Signal 2009;2:ra29. [PubMed: 19549984]
- Endoh-Yamagami S, et al. Curr Biol Aug 11;2009 19:1320. [PubMed: 19592253]
- Liem K Jr, He M, Ocbina P, Anderson K. Proc Natl Acad Sci U S A Aug 11;2009 106:13377. [PubMed: 19666503]
- Chen MH, Gao N, Kawakami T, Chuang PT. Mol Cell Biol Aug;2005 25:7042. [PubMed: 16055716]
- Merchant M, et al. Mol Cell Biol Aug;2005 25:7054. [PubMed: 16055717]
- Tay SY, Ingham PW, Roy S. Development Feb;2005 132:625. [PubMed: 15647323]
- Wolff C, Roy S, Ingham PW. Curr Biol Jul 15;2003 13:1169. [PubMed: 12867027]
- Wilson CW, et al. Nature May 7;2009 459:98. [PubMed: 19305393]
- Aanstad P, et al. Curr Biol Jun 23;2009 19:1034. [PubMed: 19464178]
- Huang P, Schier AF. Development Sep;2009 136:3089. [PubMed: 19700616]
- Sekimizu K, et al. Development Jun;2004 131:2521. [PubMed: 15115751]
- Wolff C, et al. Genes & development Jul 1;2004 18:1565. [PubMed: 15198976]
- Burglin TR, Kuwabara PE. WormBook 2006;1
- Goodrich LV, Johnson RL, Milenkovic L, McMahon JA, Scott MP. Genes & development Feb 1;1996 10:301. [PubMed: 8595881]
- Chen Y, Struhl G. Cell Nov 1;1996 87:553. [PubMed: 8898207]
- Marigo V, Scott MP, Johnson RL, Goodrich LV, Tabin CJ. Development Apr;1996 122:1225. [PubMed: 8620849]
- Kang D, et al. Development Apr;2003 130:1645. [PubMed: 12620988]
- Simonnet F, Deutsch J, Queinnee E. Dev Genes Evol Nov;2004 214:537. [PubMed: 15365834]

26. Takashima S, Mkrtchyan M, Younossi-Hartenstein A, Merriam JR, Hartenstein V. *Nature* Jul 31;2008 454:651. [PubMed: 18633350]
27. Trowbridge JJ, Scott MP, Bhatia M. *Proc Natl Acad Sci U S A* Sep 19;2006 103:14134. [PubMed: 16968775]
28. Ingham PW, McMahon AP. *Genes & development* Dec 1;2001 15:3059. [PubMed: 11731473]
29. Chiang C, et al. *Nature* Oct 3;1996 383:407. [PubMed: 8837770]
30. Preat T. *Genetics* Nov;1992 132:725. [PubMed: 1468628]
31. Gurley KA, Rink JC, Sánchez Alvarado A. *Science* Jan 18;2008 319:323. [PubMed: 18063757]
32. Iglesias M, Gomez-Skarmeta JL, Salo E, Adell T. *Development* Apr;2008 135:1215. [PubMed: 18287199]
33. Petersen CP, Reddien PW. *Science* Jan 18;2008 319:327. [PubMed: 18063755]
34. Adell T, Salo E, Boutros M, Bartscherer K. *Development* Mar;2009 136:905. [PubMed: 19211673]
35. Pedersen L, Rosenbaum J. *Curr Top Dev Biol* 2008;85:23. [PubMed: 19147001]
36. Wong SY, Reiter JF. *Curr Top Dev Biol* 2008;85:225. [PubMed: 19147008]
37. Acknowledgements: We thank the Sánchez lab for helpful comments and Carrie Adler for sharing data on *iguana*. Work supported by NIH NIGMS grant RO-1 GM57260 to ASA, and F32GM082016 to KAG. JCR was funded by the European Molecular Biology Association. ASA is a Howard Hughes Medical Institute investigator. All sequences associated with this study have been deposited in GenBank and have accession numbers GQ337474 to GQ337490.

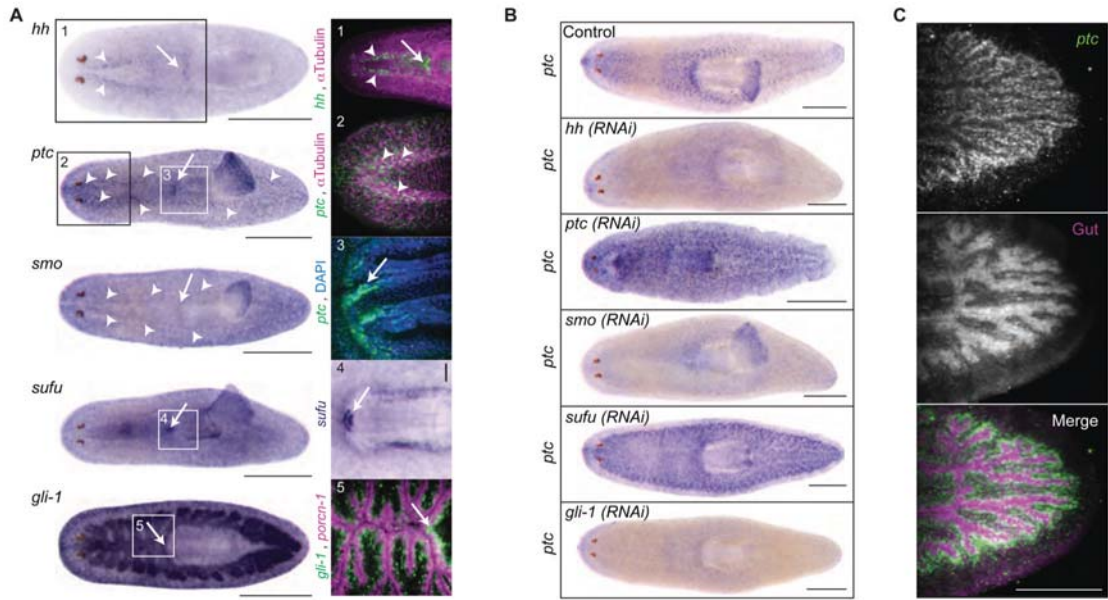


**Fig. 1.** Planarian Hedgehog signaling. **(A)** Gene expression in intact animals. Boxes magnified on right. 1: Epifluorescence image, *hh* (green), CNS (magenta, anti- $\alpha$ -Tubulin). 2: Confocal image, ventral head: *ptc* (green). CNS (magenta, anti- $\alpha$ -Tubulin). 3: Root of pharynx: *ptc* (green). Nuclei (Blue, DAPI). 4: *sufu* expression near root of pharynx. 5: *gli-1* (green), gut epithelium (magenta, *Smed-porcn-1* and *Smed-sialin*). Scale bar, 0.5 mm. Arrow heads, VNC. Arrow, root of pharynx. **(B)** *ptc* expression in RNAi-treated intact animals. The seemingly paradoxical up-regulation of *ptc* upon *ptc(RNAi)* results from the massive promotion of Hh signaling by *ptc(RNAi)*. Scale bar, 0.5 mm. **(C)** *ptc* expression confocal images in *sufu (RNAi)* intact animals. Scale bar, 0.2 mm.

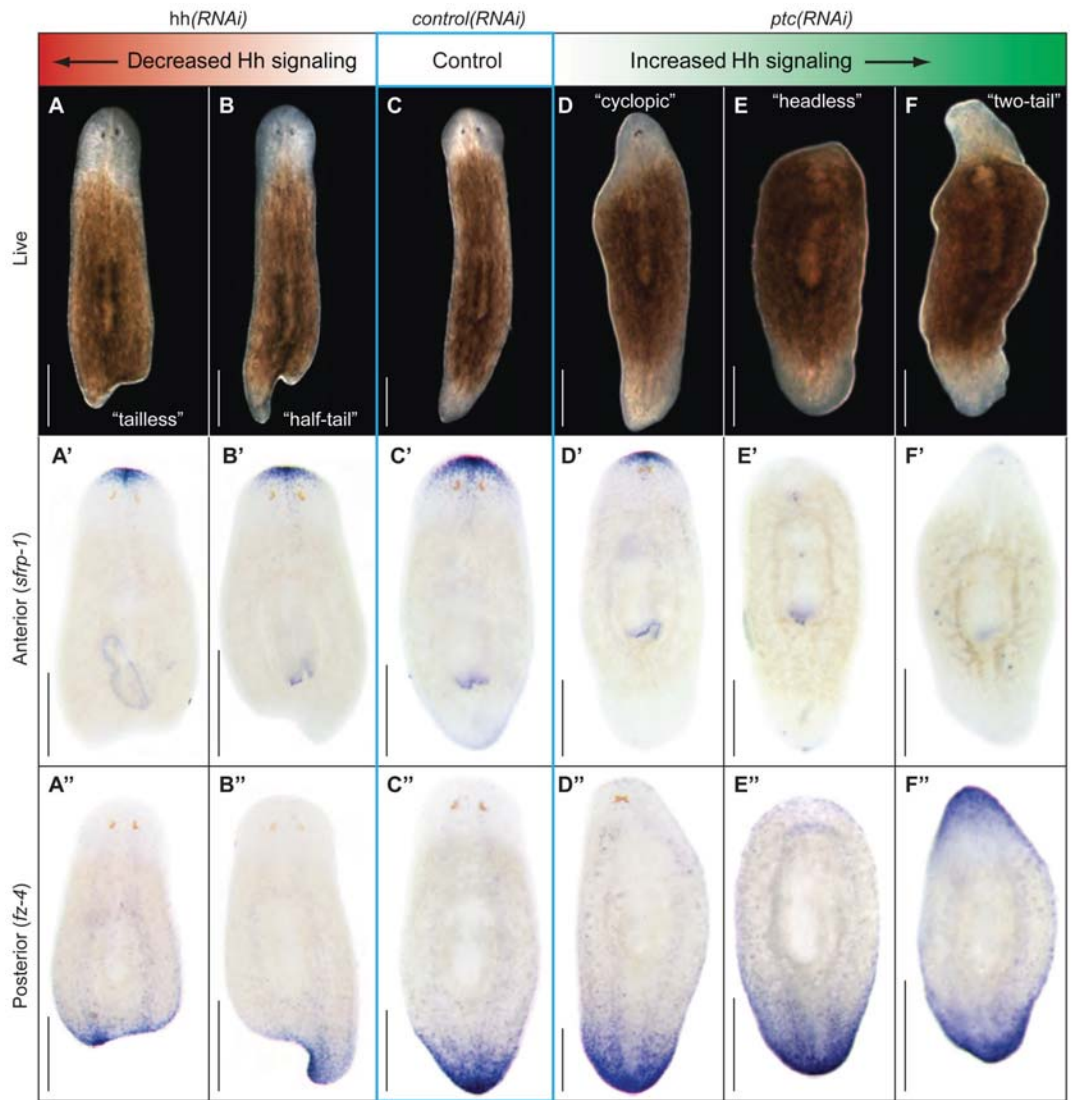


**Fig. 2.** Mis-regulated Hh signaling results in A/P patterning defects. (A–F) Live images of regenerating trunk fragments 14d after amputation. Decreased Hh signaling achieved by *hh(RNAi)* (A–B’), and increased signaling by *ptc(RNAi)* (D–F’). Phenotypes are arranged according to severity. (A’–F’). Expression of anterior marker (*Smed-sFRP-1*; (31,33)). (A’’–F’’) Expression of posterior marker (*Smed-fz-4*; (31)).

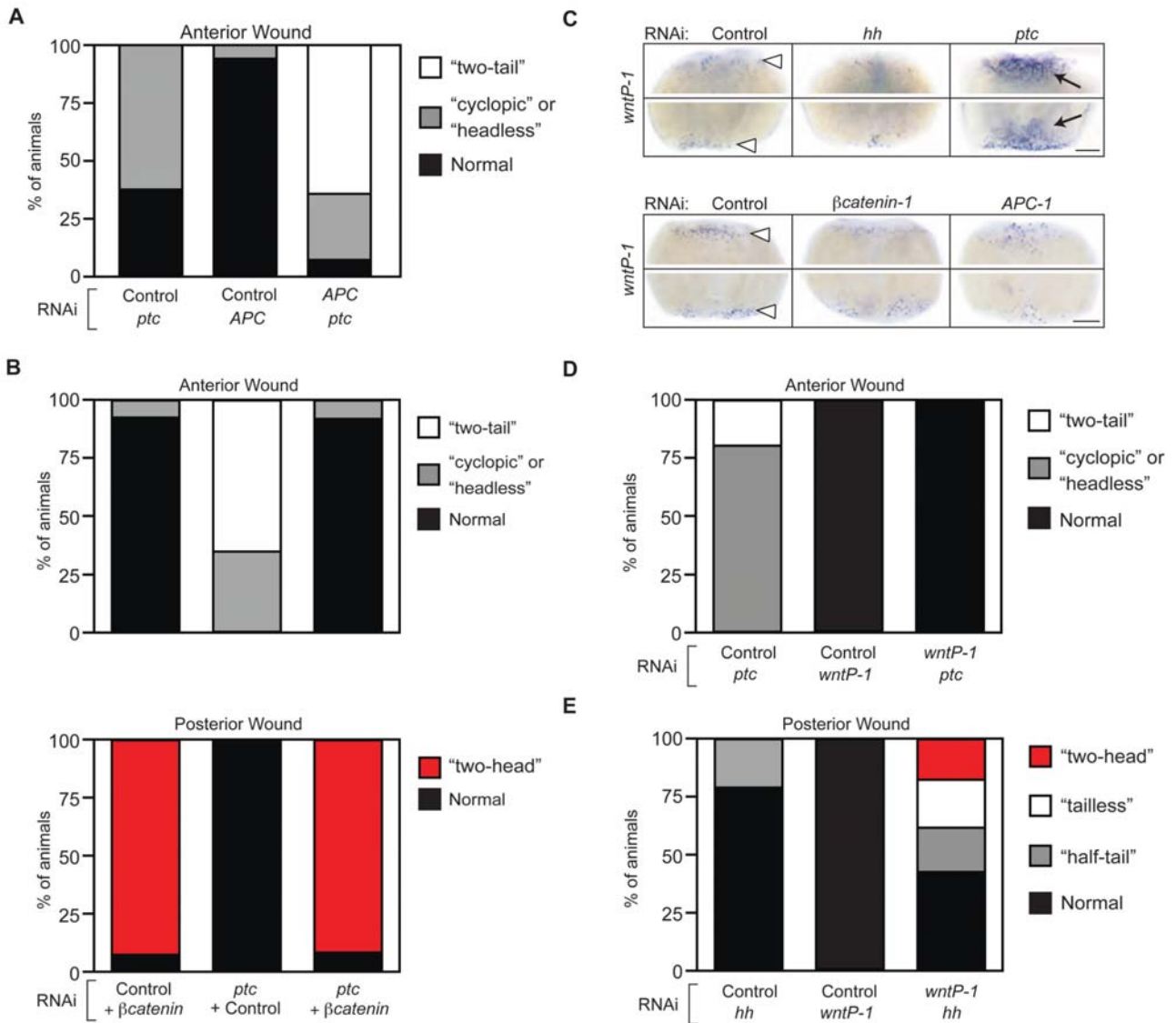


**Fig. 3.** Hh specifies A/P fate via interaction with Wnt/ $\beta$ -catenin signaling. **(A, B)** Quantification of double-RNAi experiments scored for anterior or posterior regeneration defects. Relative frequency of indicated phenotypes in a cohort of trunk fragments scored 14d after amputation. **(A)** N>15 animals/condition. **(B)** N>20 animals/condition. **(C)** *wntP-1* expression at 1d post-amputation. White arrowheads, expression at both anterior (upper panels of each set) and posterior (lower panels of each set) wounds in control animals. Black arrows, upregulated expression in *ptc*(RNAi). Scale bars, 0.2 mm. **(D, E)** Quantification of double-RNAi experiments scored for **(D)** anterior and **(E)** posterior regeneration defects. Relative frequency of indicated phenotypes in trunk fragment cohort scored 14d after amputation. N>21 animals/condition.



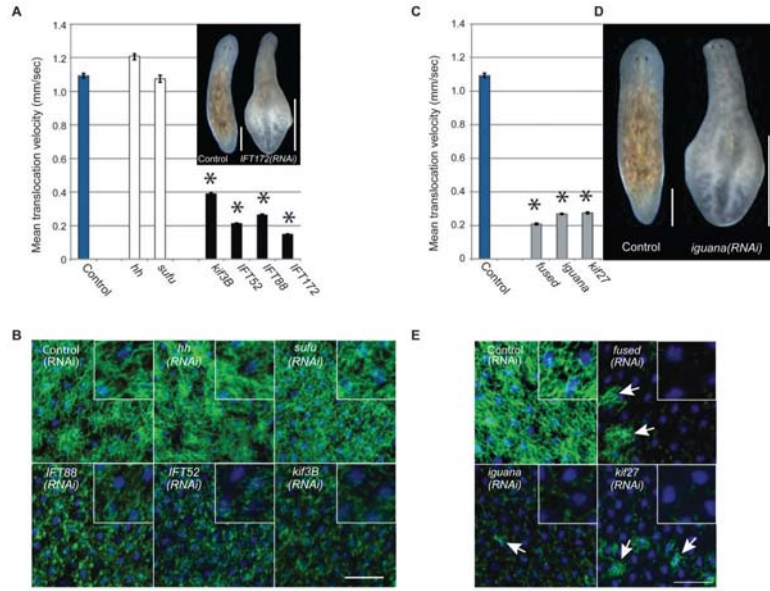


**Fig. 4.** Hh signaling is cilia-independent and *kif27*, *fused*, and *iguana* are cilia genes in planarians. **(A)** Mean translocation speed quantified from movies of animals having received the indicated RNAi-treatments. Error bars: SEM. Asterisks: p-value < 0.01 vs. control (One-way ANOVA),  $\geq 4$  movies with  $N \geq 5$  animals per movie. **Inset:** Example of tissue edema caused by *IFT172* (*RNAi*). Scale bar, 0.5 mm. **(B)** Ventral cilia confocal projections (green, anti-acetylated Tubulin), overlaid with nuclei (blue, DAPI) to demonstrate epithelial integrity. RNAi-treatments as indicated. Inset: zoom. Punctate pattern: remaining cilia stumps. Scale bar, 50  $\mu$ m. **(C)** Translocation speed calculated as in 4A. **(D)** Tissue edema in *iguana*(*RNAi*)-animal 14 days after amputation. Scale bar, 0.5 mm. **(E)** Ventral cilia confocal projections (green, anti-acetylated Tubulin) overlaid with nuclei (blue, DAPI) as in 4B. Arrows: remaining tufts of cilia on cells not yet affected by RNAi. Residual staining in *fused*(*RNAi*), *iguana*(*RNAi*), and *kif27*(*RNAi*) animals due to non-cilia related staining of sub-epithelial structures. Scale bar: 50  $\mu$ m.